Structural Engineering and Mechanics, *Vol. 73, No. 3 (2020) 303-317*
DOI: https://doi.org/10.12989/sem.2020.73.3.303

Seismic response evaluation of concentrically rocking zipper braced frames

Nasim Irani Sarand[1a] and Abdolrahim Jalali*[2]

[1]*Structural Engineering Department, School of Civil Engineering, University of Tabriz, Tabriz, Iran*
[2]*Department of Civil Engineering, Faculty of Engineering, University of Kyrenia, Girne, Mersin 10, Turkey*

(Received July 5, 2018, Revised September 10, 2019, Accepted October 11, 2019)

Abstract. In this study an innovative rocking zipper braced frame (RZBF) is proposed to overcome the deficiencies of common concentrically braced frames. RZBF is an improved rocking concentrically braced frame which is based on combination of rocking behavior and zipper columns. The base rocking joints and post-tensioned bars provide rocking response and restoring force, respectively. Also, zipper columns distribute the unbalance force over the frame height and reduce the damage concentration. To evaluate seismic performance of RZBF, a comparison study is carried out considering concentrically braced frame, zipper braced frame, rocking concentrically braced frame and RZBF. Thereby, a suite of non-linear time history analyses had been performed on four different types of archetypes with four, six, eight, ten and twelve stories. Frames were designed and non-linear time history analyses were conducted in OpenSees. To compare the seismic behavior of the archetypes, roof drifts, residual roof drifts, story drifts, the forces of first and top story braces, PT bars forces, column uplift and base shears were taken in to consideration. Results illustrate that using RZBF, can reduce the damage due to reduced residual drifts. Zipper columns enhance the seismic performance of rocking systems. As the number of stories increase in the RZBF systems, larger top story braces were needed. So the RZBF system is applicable on low and midrise buildings.

Keywords: seismic performance; rocking system; zipper column; self-centering; nonlinear time history analysis

1. Introduction

Recently, high performance lateral load resisting systems have been developed to preserve the advantages of concentrically braced frames (CBFs) while reducing structural damage and residual drifts during severe earthquakes. In this relation, studies on seismic performance of different systems were conducted such as buckling restrained braced frames (BRBFs) (Fahnestock *et al*. 2003), zipper braced frames (ZBFs) (Yang *et al*. 2008b) and rocking concentrically braced frames (RCBFs) (Roke *et al*. 2009, Wiebe *et al*. 2013). One of the lateral load resisting systems for ductile seismic behavior is BRBFs, which consist of two basic components: the first component is steel core blocked by a hollow steel section and the second component is the confining material. Although, BRBFs had better seismic performance than CBFs in terms of inter story drifts (Sabelli *et al*. 2003), they are prone to have large residual drifts as a result of low post-yield stiffness (Kiggins and Uang 2006, Ariaratana and Fahnestock 2011). The other lateral load resisting system with improved seismic behavior is zipper braced frames (ZBFs) which was proposed by Khatib *et al*. (1998). Zipper columns were added at the midpoint of the bay of CBF systems to redistribute the unbalanced force over the frames height. In other words, zipper columns help to mobilize the stiffness of the braces those left and all the beams to resist undesired unbalanced forces, which prevent concentration of damage in a single story. Many researchers had different studies in accordance with ZBFs systems. Sabelli *et al*. (2001), showed the efficiency of zipper columns in terms of uniform distribution of the inter story drift over the frame height. Yang *et al*. (2008a) suggested the modified zipper braced frames (suspended zipper braced frame) and conducted nonlinear time history analyses. In the proposed refined system the top hat truss was added across the zipper columns which prevent the formation of a full plastic mechanism due to supplying a larger deformation capacity. The deficiency of the modified ZBF is with increasing the number of stories, the cross section for top story braces extremely increase. Ozcelik *et al*. (2016) showed that the modified ZBF had poor performance comparing with ordinary CBF in high rise buildings considering column axial load demand.

In the last lateral load resisting system, concept of rocking behavior at the base joint was used to improve the seismic behavior. There are numerous studies in relation with rocking systems such as using rocking behavior concept at the bridge pier (Beck and Skinner1974, Pollino and Bruneau 2007and 2010), rocking unbounded post tensioned concrete wall (Kurama *et al*. 1999a and 1999b), rocking steel frames (Clough and Huckelbridge 1997, Kelly and Tsztoo 1977), rocking core system (Wu and Lu 2015, Belbo and Roke 2015 and 2018) and using rocking system in retrofitting of existing steel structures (Mottier *et al*. 2018). Beck and Skinner (1974), studied on the rocking A-shaped bridge pier. They illustrated that the maximum

*Corresponding author, Assistant Professor
E-mail: jalali@tabrizu.ac.ir;
jalali.abdolrahim@kyrenia.edu.tr
[a] Ph.D. Candidate

ISSN: 1225-4568 (Print), 1598-6217 (Online)

displacement of the rocking pier was larger than the fixed-base ones. Pollino and Bruneau (2007) used rocking steel piers in retrofitting bridges. They conducted nonlinear time history analysis and found that uplift of pier can affect the effective weight as a result of exciting the vertical mode of the pier. In the other experimental study, they found that due to rocking behavior of the four-legged bridge steel truss pier, it self-centered after large lateral displacement (3.9%) (Pollino and Bruneau, 2010). Using rocking concept at the unbounded post tensioned concrete wall was proposed by Kurama *et al*. (1999a, 1999b). According to the findings of Kurama *et al*. (1999a),in comparison with ordinary cast-in-place concrete walls, rocking post tensioned concrete walls experience larger drifts due to rocking behavior and smaller residual drift as a result of self-centering induced by post tensioned bars.

The first study of a rocking steel frame was conducted by Clough and Huckelbridge (1997) who performed an experimental study on a three story frame with rocking column base. They showed that the local strain ductility demand can reduce by rocking behavior. In the other study, using yielding steel bars along with the rocking base was proposed by Kelly and Tsztoo (1977) to dissipate energy during the column uplift. The results were in consistent with the results of Clough and Huckelbridge (1977). Post tensioned moment resisting frame was developed by Ricle *et al*. (2001) in order to increase the ductility capacity without damage. Garlock *et al* (2005), Rojas *et al*. (2005), Lin *et al*. (2009) and Wolski *et al*. (2009) conducted different researches on post tensioned beam-column connections which provide rocking behavior. Light-weight energy dissipating rocking core frame was proposed as a new lateral load resisting system by Wu and Lu (2015). In this system, due to using self-centering energy-dissipating braces, seismic response in term of low residual drifts has enhanced. Rocking core system with the intent of providing considerable drift capacity and limited structural damage and residual drifts was suggested by Belbo and Roke (2015 and 2018).

Rocking concentrically braced frames was proposed by Roke *et al*. (2006) as a high performance lateral load resisting system for steel structures. Special details at the column to base joint provide the rocking behavior and the restoring force is provided through the post tensioned bars. Sause *et al*. (2006) and Roke *et al*. (2009) conducted several nonlinear static and dynamic analyses on the different six story RCBF configuration in order to evaluate the seismic performance and find the optimum configuration. Recent studies on RCBFs, such as RCBF with energy dissipating elements (Tremblay 2008, Christopoulos *et al*. 2008, Zhu and Zhag 2008, Chancellor *et al*. 2014), RCBF with different configuration (Sause *et al*. 2010, Roke *et al*. 2012), using multiple rocking joints over the frame height (Wiebe *et al*. 2013), dual RCBFs (Eatherton *et al*. 2014, Rahgozar *et al*. 2016 and 2017) and tension-only braced frames with rocking core (Hu *et al*. 2018), showed that the RCBFs are capable of reducing damage under higher level of lateral loads and improve the seismic response of the CBFs in terms of uniform distribution of inter story drifts. Roke *et al*. (2012) showed that by increasing the frame width of the RCBF system, higher modes effects decrease. The experimental tests which were performed by Eatherton *et al*. (2014) showed that rocking system is able to diminish residual drift after sever earthquakes. Chancellor *et al*. (2014) evaluated seismic performance of the RCBF system with ED elements considering different number of stories. The numerical results illustrated with increasing the height of the RCBF, the first assumption about overturning moment was disaffirmed (Chancellor *et al*. 2014). The rocking performance at the base of RCBFs leads to larger lateral displacement and limited member force demand as a result of softening mechanism of RCBF (Dyanati *et al*. 2017). Huang *et al*. (2018) showed that RCBFs are economically better systems than CBFs for low and mid-rise buildings under severe earthquakes.

Despite different studies on the various types of RCBF, this system may experience concentration of unbalance force in the braces of top stories (Roke *et al*. 2006, 2009). For enhancing the behavior of RCBF in terms of distribution of the unbalanced force, in this study zipper columns are proposed to use at the mid bay along the post-tensioned bars in RCBF system. In the proposed rocking zipper braced frame (RZBF), zipper columns connect the mid points of the bay together and convey the undesired unbalance force. In order to investigate the seismic behavior of RZBF, a comparative study with other archetypes (CBF, ZBF, RCBF) under a set of far field ground motions is conducted considering different seismic behavior such as roof drift ratio, residual roof drift ratio, gap opening, force of post-tensioned bars and top story braces.

2. Methodology

To assess seismic performance of RZBF and compare the behavior with the other systems, four different office buildings with 4, 6, 8, 10 and 12 story were designed. OpenSees software (McKenna *et al*. 2000) was used to conduct nonlinear time history dynamic analyses.

2.1 Frame configuration

In order to evaluate the seismic response of the RZBF, four different archetypes were studied in this work. The layouts of the frames are presented in Fig. 1. Figs. 1(a)-(d), present four-story CBF, ZBF, RCBF and RZBF, respectively. ZBF and RZBF are the improved forms of CBF and RCBF. In order to redistribute the damage over the height of frames and prevent the concentration of damage in one story, zipper columns were used.

As shown in Figs. 1(c)-(d), base struts were used between column bases in rocking frames, with the aim of conveying the base shear from the uplifted column to the column in continuity with the foundation. There are two additional gravity columns, adjacent to the column of the rocking frame, which distribute the gravity load induced by the rocking behavior of the systems. Also, energy dissipating (ED) elements are used over the height of rocking frames and located between the gravity columns and columns of rocking frames

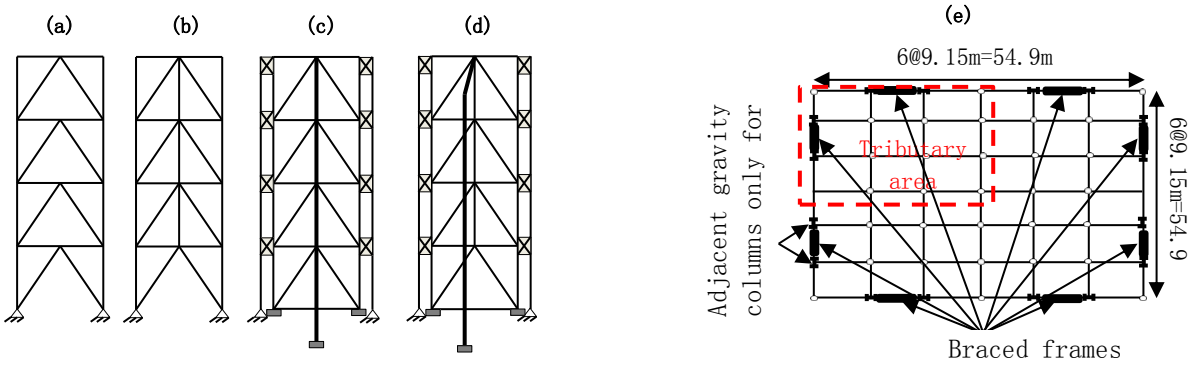

(a) CBF (b) ZBF (c) RCBF (d) RZBF (e) Floor plan for prototype structure

Fig. 1 Archetypes configuration and floor plan

2.2 Prototype structures

The floor plans of prototype structure consist of 6 bays in width and length (as presented in Fig. 1(e)). The bay length is 9.15 m, the height of first story is 4.5 m and the other stories height is 3.9 m. Dead load plus the weights of partitions constitute the seismic mass. The tributary seismic mass values for the first, second, third and roof stories are 378000, 375000, 375000 and 258000 kg, respectively.

Office buildings located in California were designed using "AISC load and resistance factor design" (2010) procedure and "Seismic provisions for structural steel buildings" (2010). A design acceleration spectrum (SA_{DS}) is generally determined assuming 5% for damping ratio. The spectral acceleration (SA) at periods of 0.2 second (SS) and SA at a period of 1 second (S1) is 1.5g and 0.6g, respectively. The site class considered to be class D and the long-period transition period (TL) assumed to be 8. So, in order to define the SA_{DS} for design base earthquake (DBE), the mentioned parameters were used.

Design steel yield strength, the modulus of elasticity and Poisson ratio was considered to be 345 MPa, 200 GPa and 0.3 respectively. For PT bars the modulus of elasticity was 205GPa, the design yield strength and ultimate strength was 454 kN and 567 kN, respectively and the Poisson ratio was 0.3. The initial PT bar forces are considered to be 40% of the yield strength for both types.

2.3 Design of archetypes

There are different design methods for rocking frames, such as equivalent lateral force seismic design procedure, response spectrum analysis seismic design procedure and the design procedure proposed by Roke *et al*. (2009). Due to elastic behavior consideration for rocking frames, the inelastic deformations do not limit the higher mode responses. Accordingly, the equivalent lateral force seismic design procedure may not be suitable method for designing the rocking systems. Since ductility demands for rocking frames are greater than ductility demands for fixed base frames and due to dependence of the ductility demands on the structural properties, using simple displacement amplification factor C_d (ASCE 7-10) for rocking frame is not proper.

The method proposed by Roke *et al*. (2009) is a modified form of the response spectrum analysis procedure for rocking frames. According to the performance-based design procedure proposed by Roke *et al*. (2009), two seismic intensity levels (design basis earthquake (DBE) and maximum considered earthquake (MCE)) were taken in to consideration. The performance objectives of immediate occupancy (IO) and collapse prevention (CP) were the corresponding performance objectives for DBE and MCE, respectively. Due to self-centering behavior of the rocking systems, the limit states of column uplift and limited PT bar yielding provide the IO performance level. The CP performance level should be conformed by the significant member yielding limit state. The summary of the Roke *et al*. (2009) proposed method is described as follow: first of all, member size, number and area of PT bars, r_{PT} ($\frac{PT_0}{PT_Y}$) and μ were defined. Then the modal properties such as first mode effective modal mass (M_1), the total mass tributary to the rocking frame (M_{total}), modal contribution factor (Γ_n), modal periods (T_n) and mode shapes ($\varnothing_n$) were calculated using a fixed base linear elastic model. M_1, M_{total} and Γ_n are calculated as:

$$M_1 = \frac{\left(\{\Phi_1\}^T[m]\{i\}\right)^2}{\left(\{\Phi_1\}^T[m]\{\Phi_1\}\right)} = \Gamma_1\left(\{\Phi_1\}^T[m]\{i\}\right) \quad (1)$$

$$M_{total} = \{i\}^T[m]\{i\} \quad (2)$$

$$\Gamma_n = \frac{\left(\{\Phi_n\}^T[m]\{i\}\right)}{M_n} \quad (3)$$

Where:

[m]= matrix of seismic mass

{i}= influence vector

The overturning moment at decompression limit state (OM_D) and PT bar yield limit state (OM_Y) determine as:

$$OM_D = \frac{\left(PT_0 + W_{rockingframe}\right)\frac{b_{rockingframe}}{2} + V_{ED}.b_{rockingframe}}{1-\eta} \quad (4)$$

$$OM_Y = \frac{\left(PT_Y + W_{rockingframe}\right)\frac{b_{rockingframe}}{2} + V_{ED}.b_{rockingframe}}{1-\eta} \quad (5)$$

$$\eta = \frac{\mu.b_{ED}}{h_1^*} \quad (6)$$

Where:

μ = friction coefficient in the lateral load bearings

$b_{rocking\ frame}$ = centerline distance between rocking columns

b_{ED} = sum of $b_{rocking\ frame}$ and centerline between rocking columns and adjacent gravity columns

h_1^* = first mode effective height

$w_{rocking\ frame}$ = weight of the rocking frame

V_{ED} = force of the supplemental constant force energy dissipation elements

Then, the design response modifications can be calculated as:

$$R_A = \frac{OM_{Elastic}}{OM_D} \quad (7)$$

$$R_{AD} = \frac{OM_{Elastic}}{OM_{D,1}} \quad (8)$$

Where R_A is a response modification factor for rocking frame and R_{AD} is a modified response modification factor to consider only first mode mass and $OM_{Elastic}$ is an elastic overturning moment which is computed using equivalent lateral forces method and R=1.

The modal member force design demands ($F_{n,x,dd}$) are calculated by using first mode design spectral acceleration ($\alpha_{y,1}$) and design spectral acceleration from elastic design spectrum at period T_n ($SA_{DS,n}$) to compute the values of lateral forces of each modes ($\{F_{m,n}\}$). Then for calculating $\{F_{n,x,dd}\}$ for higher modes, the defined lateral forces, are applied to a fixed base model. Lateral force of each mode defined as:

$$\{F_{m,n}\} = \Gamma_n [m]\{\Phi_n\} SA_{DS,n} \quad (9)$$

By applying modal load factor to $\{F_{n,x,dd}\}$, the factored member force design demands $\{F_{fn,x,dd}\}$ is determined by combining Roke *et al*. (2009) correlation coefficients and CQC method the total factored member force design demand are determined. The Roke *et al*. (2009) proposed correlation coefficient is expressed as:

$$\rho_m = \begin{cases} 1 & if \quad i = n \\ 0.25 & if \quad i \neq n \end{cases} \quad (10)$$

After that the estimated overturning moment under DBE (OM_{DBE}) is calculated using estimated peak lateral roof drift design demand under DBE (θ_{DBE}). Iterative calculation of β_E is conducted using OM_{DBE} and θ_{DBE} until the iteration values difference become small. The summary of rocking frame design procedure is presented schematically in Fig. 2.

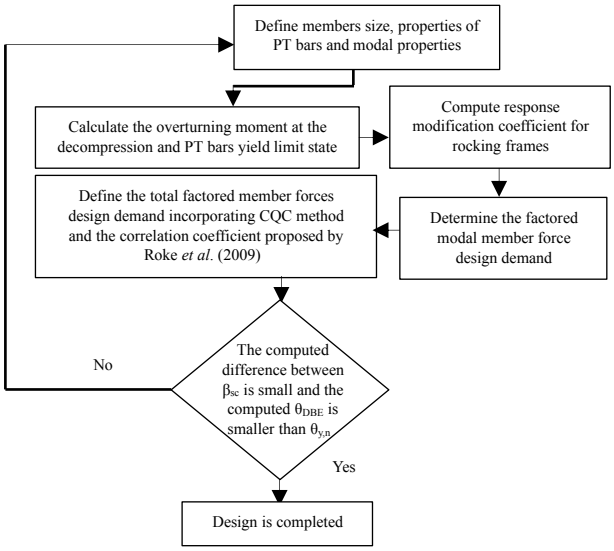

Fig. 2 Summary of the design process of rocking frames

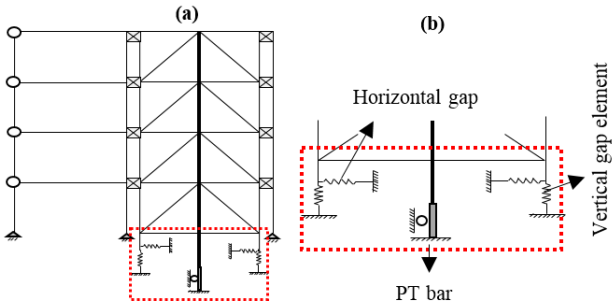

(a) Elevation view (b) Details of boundary conditions for gap elements and PT bars connections

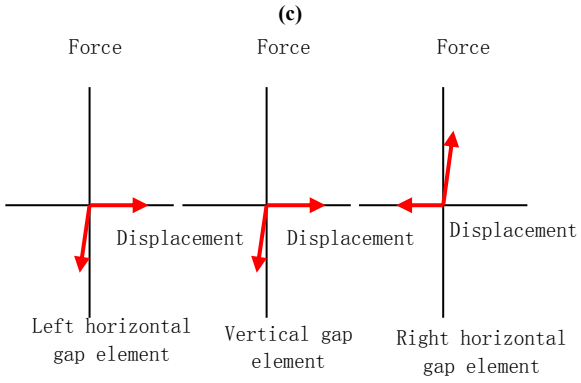

(c) Behavior of gap element

Fig. 3 Numerical model of rocking frames

Also, the design method proposed by Yang *et al*. (2008) was used for designing suspended zipper braced frames (ZBF). Design of ZBF consists of two steps: step 1) the frame is sized to resist the actions which result from the gravity and lateral load applied to CBF (ordinary concentrically braced frame without zipper columns). In this phase the brace sizes in all stories except top story are fixed. Step 2) in this phase zipper columns are added and other structural elements are redesigned except braces below the top story. The member size for fixed base frames and rocking frames are presented in Tables 1-2, respectively.

Table 1 Member size for CBF and ZBF systems

	CBF			ZBF			
Story	Column	Beam	Brace	Column	Beam	Brace	Zipper column
1	W10X106	W12X106	W12X120	W12X136	W10X60	W12X190	-
2	W10X106	W12X96	W12X96	W12X120	W10X60	W12X96	W12X58
3	W12X96	W12X96	W12X106	W12X106	W12X120	W12X120	W12X106
4	W12X96	W12X96	W12X87	W12X58	W8X48	W12X190	W12X152
1	W14X145	W12X106	W14X90	W12X190	W10X54	W12X152	-
2	W14X145	W12X96	W14X90	W12X152	W10X49	W12X152	W10X54
3	W14X90	W12X96	W14X109	W12X136	W10X49	W12X120	W12X106
4	W14X90	W12X96	W14X109	W12X136	W10X39	W12X120	W12X152
5	W14X68	W12X96	W14X159	W12X120	W12X136	W12X72	W12X170
6	W14X68	W12X106	W14X90	W12X53	W10X33	W12X190	W12X210
1	W14X283	W12X106	W12X106	W14X342	W10X77	W12X190	-
2	W14X257	W12X96	W12X96	W14X283	W10X60	W12X190	W10X68
3	W14X159	W12X106	W12X79	W12X279	W10X60	W12X170	W12X136
4	W14X159	W12X96	W12X65	W12X252	W10X49	W12X170	W12X190
5	W14X132	W12X96	W12X65	W12X252	W10X49	W12X170	W14X233
6	W14X132	W12X96	W12X79	W12X210	W10X33	W12X136	W14X257
7	W14X109	W12X96	W12X79	W12X210	W14X233	W12X96	W14X311
8	W14X109	W12X96	W12X87	W12X96	W10X33	W12X305	W14X342
1	W14X311	W12X96	W12X152	W14X426	W10X77	W12X170	-
2	W14X283	W12X96	W12X136	W14X370	W10X68	W12X170	W10X77
3	W14X283	W12X106	W12X136	W14X370	W10X68	W12X152	W12X152
4	W14X211	W12X96	W12X120	W14X342	W10X60	W12X152	W12X230
5	W14X211	W12X106	W12X79	W14X342	W10X54	W12X152	W14X283
6	W14X193	W12X96	W12X79	W14X311	W10X49	W12X120	W14X342
7	W14X193	W12X96	W12X96	W14X311	W10X45	W12X120	W14X398
8	W14X145	W12X96	W12X96	W14X283	W10X33	W12X96	W14X455
9	W14X145	W12X96	W12X136	W14X283	W14X311	W12X96	W14X500
10	W14X109	W12X96	W12X136	W14X132	W10X33	W14X455	W14X550
1	W14X455	W12X96	W12X152	W14X500	W10X77	W14X455	-
2	W14X455	W12X96	W12X152	W14X500	W10X77	W14X370	W10X77
3	W14X311	W12X106	W12X152	W14X455	W10X77	W14X370	W12X152
4	W14X311	W12X96	W12X152	W14X455	W10X68	W14X283	W12X230
5	W14X283	W12X106	W12X120	W14X426	W10X68	W14X211	W14X311
6	W14X283	W12X96	W12X96	W14X398	W10X68	W12X152	W14X370
7	W14X283	W12X96	W12X79	W14X398	W10X49	W12X120	W14X426
8	W14X257	W12X96	W12X79	W14X370	W10X49	W12X120	W14X500
9	W14X233	W12X96	W12X79	W14X370	W10X49	W12X152	W14X550
10	W14X233	W12X210	W14X99	W14X370	W10X33	W14X159	W14X605
11	W14X90	W12X96	W14X145	W14X342	W14X455	W14X370	W14X605
12	W14X90	W12X96	W14X99	W14X159	W10X33	W14X550	W14X665

Table 2 Member size for RCBF and RZBF systems

	RCBF			RZBF			
Story	Column	Beam	Brace	Column	Beam	Brace	Zipper column
1	W12X170	W12X106	W12X170	W14X283	W10X60	W12X152	-
2	W10X170	W12X96	W12X106	W14X283	W10X60	W12X120	W12X106
3	W12X106	W12X96	W12X152	W12X106	W12X120	W12X170	W12X136
4	W12X106	W12X96	W12X106	W12X58	W8X48	W14X211	W12X152
1	W14X211	W12X106	W14X233	W12X279	W10X54	W12X190	-
2	W14X211	W12X96	W14X176	W12X230	W10X49	W12X170	W14X233
3	W14X193	W12X96	W12X96	W12X230	W10X49	W12X106	W14X176
4	W14X193	W12X96	W14X74	W12X230	W10X39	W12X106	W12X96
5	W14X68	W12X96	W14X193	W12X120	W12X136	W12X96	W14X74
6	W14X68	W12X106	W12X96	W12X53	W10X33	W12X366	W12X96
1	W14X130	W12X106	W14X257	W14X500	W10X77	W14X283	-
2	W14X342	W12X96	W14X193	W14X455	W10X60	W14X283	W12X190
3	W14X311	W12X106	W14X132	W14X455	W10X60	W14X1159	W12X252
4	W14X311	W12X96	W12X96	W14X455	W10X49	W14X132	W14X336
5	W14X311	W12X96	W12X96	W14X370	W10X49	W14X132	W14X398
6	W14X193	W12X96	W12X152	W14X370	W10X33	W14X120	W14X455
7	W14X193	W12X96	W12X152	W14X370	W14X233	W14X132	W14X550
8	W14X193	W12X96	W12X190	W14X176	W10X33	W14X455	W14X550
1	W14X455	W12X96	W14X370	W14X730	W10X77	W14X370	-
2	W14X426	W12X96	W14X311	W14X730	W10X68	W14X370	W14X90
3	W14X426	W12X106	W14X233	W14X730	W10X68	W14X193	W14X311
4	W14X342	W12X96	W14X1159	W14X665	W10X60	W14X159	W14X398
5	W14X342	W12X106	W12X106	W14X665	W10X54	W14X159	W14X500
6	W14X342	W12X96	W12X106	W14X605	W10X49	W14X159	W14X665
7	W14X342	W12X96	W12X170	W14X605	W10X45	W14X159	W14X665
8	W14X211	W12X96	W12X170	W14X550	W10X33	W14X99	W14X730
9	W14X211	W12X96	W12X210	W14X550	W14X311	W14X99	W14X730
10	W14X211	W12X96	W12X210	W14X257	W10X33	W14X730	W14X730
1	W14X730	W12X96	W14X455	W14X730	W10X77	W14X500	-
2	W14X730	W12X96	W14X370	W14X730	W10X77	W14X455	W14X370
3	W14X455	W12X106	W14X370	W14X730	W10X77	W14X342	W14X370
4	W14X455	W12X96	W14X283	W14X730	W10X68	W14X283	W14X426
5	W14X455	W12X106	W14X211	W14X730	W10X68	W14X211	W14X426
6	W14X455	W12X96	W12X152	W14X730	W10X68	W12X193	W14X550
7	W14X455	W12X96	W12X120	W14X665	W10X49	W12X176	W14X605
8	W14X455	W12X96	W12X120	W14X665	W10X49	W12X176	W14X605
9	W14X370	W12X96	W12X152	W14X665	W10X49	W12X176	W14X665
10	W14X370	W12X210	W14X159	W14X550	W10X33	W14X132	W14X665
11	W14X132	W12X96	W14X370	W14X550	W14X455	W14X90	W14X730
12	W14X132	W12X96	W14X132	W14X257	W10X33	W14X730	W14X730

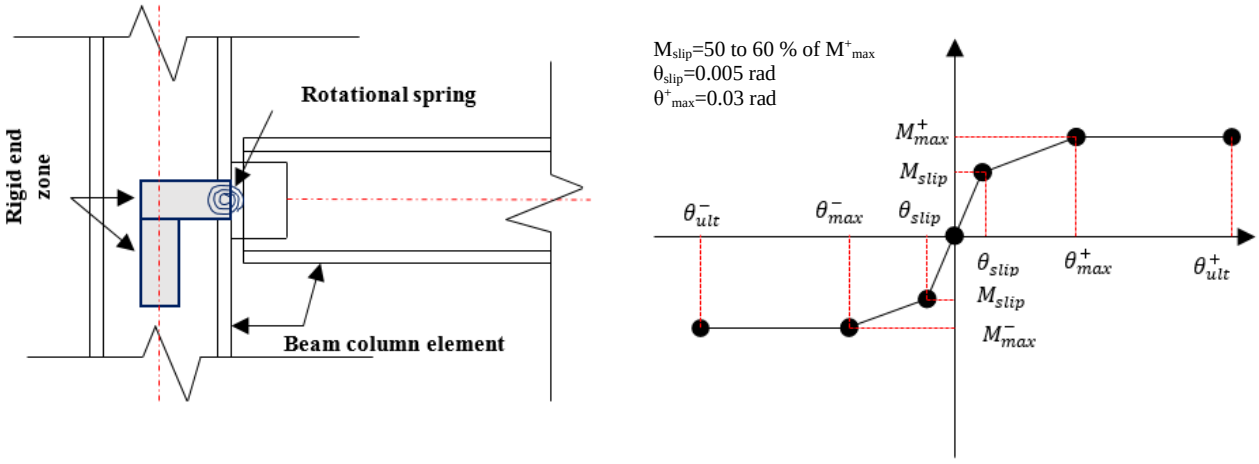

(a) OpenSees model for shear tab connection (b)

Fig. 4 Schematic model and moment rotation behavior for shear tab connection

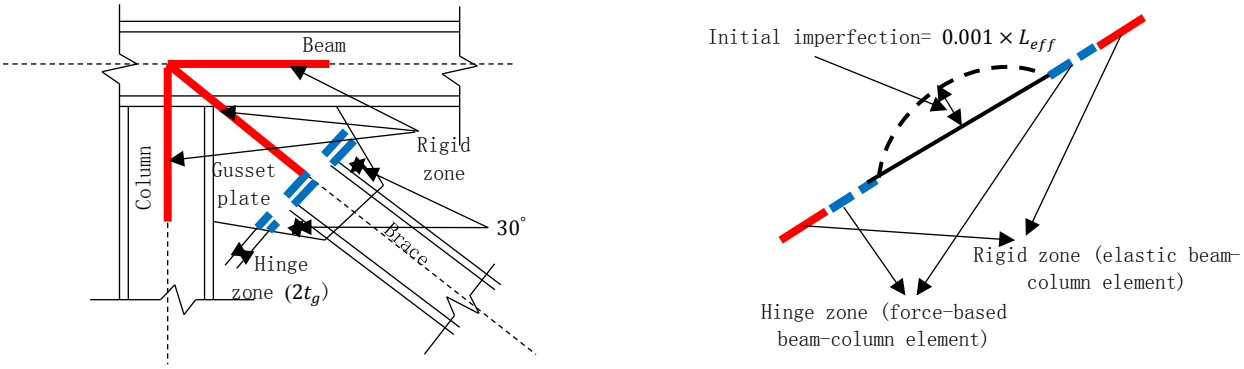

(a) Details of gusset plate connection (b)Numerical model of brace

Fig. 5 Gusset plate connection and brace numerical model

2.4 Analytical model

The seismic performances of the archetypes were evaluated by nonlinear time history analysis using OpenSees software (McKenna *et al*. 2000). Figs. 3(a)-(c) show the two dimensional analytical model and the details of boundary conditions and the behavior of gap elements used in the analytical model, respectively. For modeling the column base connections of the rocking frames, Elastic Perfectly Plastic Gap (EPP Gap) elements with elastic-no-tension material were used in horizontal and vertical directions. By using Elastic PP material parallel with elastic material, ED elements were modeled. As shown in Fig. 3(b), the base gap connections are shown by horizontal and vertical springs. Leaning columns (LC) were used with the intent of modeling P-Δ effects and for modelling LC, Elastic-beam-column elements were used. Structural members such as beams, columns and braces were modeled using forced-based nonlinear beam-column elements with four integration points based on Gauss-Lobatto quadrature and Steel02 material for fiber sections. To model gradual yielding of wide flange sections, eight and four fibers were used over the height and through the flange thickness, respectively. Beam-column connections for concentrically braced frames (CBF) and zipper braced frames (ZBF) were modeled as pin connection. Beam-column connections in the rocking frames were shear tab types that in the numerical modeling concentrated rotational spring element was used (Liu and Astaneh-asl 2004), as shown in Fig. 4(a). Shear tab connection is a combination of zero-length element with hysteretic material with pinching response (Liu and Astaneh-Asl, 2004). The moment-rotation model developed by Liu and Astaneh-Asl (2004), was utilized to estimate the maximum positive and negative moment capacities and rotational stiffness for shear tab connections (Fig. 4(b)).

For modeling buckling behavior of braces, 2 force-based elements (Uriz *et al*., 2008) or 10 force-based elements were proposed (Gunnarson 2004, Terzic 2013). In this study, braces are divided in to 10 nonlinear beam-column elements with three integration points. The initial imperfection used in the modeling was 0.001 of its effective length. In order to model PT bars, corotational truss elements were used with a combined material consisting of elastic perfectly plastic and hardening material to simulate the tension-only behavior. Gusset plates could be modeled with different methods such as rotational springs (Hsiao *et al*. 2012, Hsiao *et al* 2013) and force-based fiber elements (Uriz 2008). The gusset plate is modeled using a combination of elastic beam-column element (rigid zone at

Table 3 Properties of ground motion set

Records	Event	Year	Station	Fault type	Magnitude	Component	Dist(Km)
r1	Imperial Valley-06	1979	Brawley Airport	Strike Slip	6.53	315	8.54
r2	Imperial Valley-06	1979	Chihuahua	Strike Slip	6.53	282	7.29
r3	Imperial Valley-06	1979	Delta	Strike Slip	6.53	262	22.03
r4	Imperial Valley-06	1979	Delta	Strike Slip	6.53	352	22.03
r5	Imperial Valley-06	1979	ElCentro Array #4	Strike Slip	6.53	140	4.90
r6	Superstition Hills-02	1987	Westmorland Fire Station	Strike Slip	6.54	090	13.03
r7	Loma Prieta	1989	Hollister Diff. Array	Reverse Oblique	6.93	165	24.52
r8	Loma Prieta	1989	Oakland – Outer Harbor wharf	Reverse Oblique	6.93	000	74.16
r9	Northridge-01	1994	Arleta - Nordhoff Fire station	Reverse	6.69	360	3.3
r10	Kobe, Japan	1995	Abeno	Strike Slip	6.90	090	24.85
r11	Kobe, Japan	1995	Amagasaki	Strike Slip	6.90	000	11.34
r12	Kobe, Japan	1995	Amagasaki	Strike Slip	6.90	090	11.34
r13	Kobe, Japan	1995	Morigawachi	Strike Slip	6.90	090	24.78
r14	Kobe, Japan	1995	Shine - Osaka	Strike Slip	6.90	000	19.14
r15	Chi-Chi, Taiwan	1999	CHY015	Reverse Oblique	7.62	W	38.14
r16	Chi-Chi, Taiwan	1999	HWA019	Reverse Oblique	7.62	N	51.87
r17	Chi-Chi, Taiwan	1999	HWA048	Reverse Oblique	7.62	N	47.36
r18	Chi-Chi, Taiwan	1999	HWA048	Reverse Oblique	7.62	W	47.36
r19	Chi-Chi, Taiwan	1999	ILA013	Reverse Oblique	7.62	N	81.71
r20	Hector Mine	1999	Amboy	Strike Slip	7.13	090	41.82
r21	Hector Mine	1999	Amboy	Strike Slip	7.13	360	41.82
r22	Hector Mine	1999	Mecca – CVWD Yard	Strike Slip	7.13	090	91.96

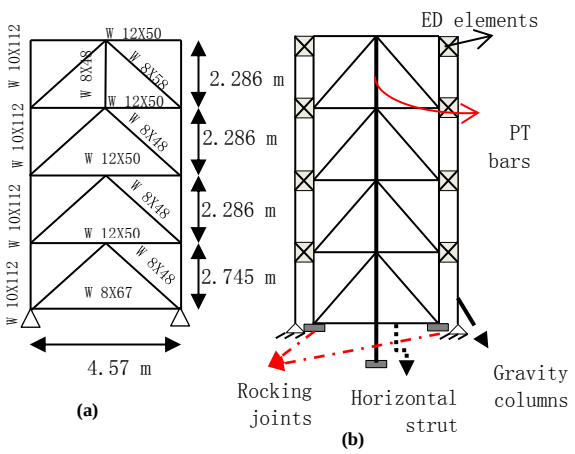

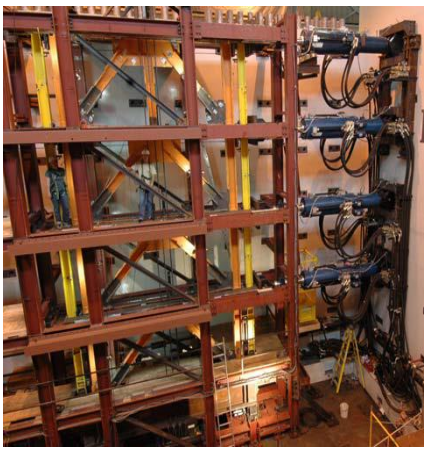

(a) Section properties of the test structure (b) Numerical model (c) Test structure (Sause *et al*. 2010)

Fig. 6 Details of test structure

the intersection of beam-column-braces) and forced-base beam-column elements (hinge zone ($2t_g$)) with two integration points. Figs. 5(a)-(b) show the schematic form of the gusset plate connection and the numerical model, respectively.

2.5 Ground motion records

A set of twenty two scaled ground motions with design-based earthquake level was used to assess the seismic behavior of the different archetypes. In order to match

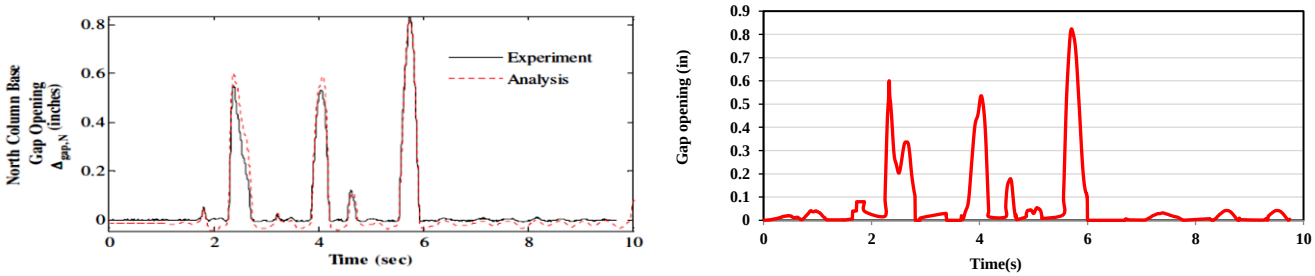

(a) Experimental result (Sause *et al*. 2010) (b) Numerical result

Fig. 7 Gap opening results

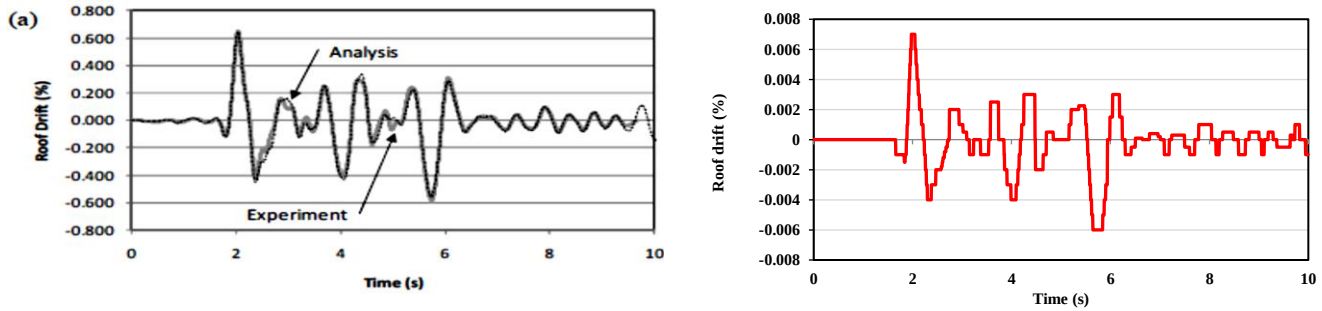

(a) Experimental result (Sause *et al*. 2010) (b) Numerical result

Fig. 8 Roof drift ratio results

SA_{DS} over a broad period range of 0.3 to 7.0 seconds, the ground motions were scaled by the Baker's proposed method. Rayleigh damping with a 5% damping ratio in the first and third modes was used. The properties of ground motions are given in Table 3.

3. Results and discussions

3.1 Validating the numerical model

The 0.6-scale experimental frame proposed by Sause *et al*. (2010) was modeled to validate the accuracy of analytical model used for rocking frames (Fig. 6(c)). A prototype frame is a 4-story office building designed for stiff site in Van Nuys, California (Sause *et al*. 2010). The test structure consists of one rocking frame with the adjacent gravity columns (Fig. 6(c)). The seismic mass from the first story to the roof, are: 135900 kg, 134800 kg, 134800 kg, and 142200 kg. The tributary gravity loads of the test structure from the first story to the roof, are: 1495 kN, 1484 kN, 1484 kN, and 1556 kN. The section properties for test structure are given in Fig. 6(a). Also, validation frame is modeled in OpenSees as Fig. 6(b). The gravity columns and base strut sections of the test structure are W8X67 and W36X230, respectively. The elements used for the numerical model is the same as elements discussed in section 2.4. Figs.7 and 8 show the results of analytical model comparing with the experimental results in terms of column uplift value and roof drift ratio, respectively. As shown in Figs. 7 and 8, there is good agreement between the results of experimental model and the analytical model.

3.2 Story drift ratio

Figs. 9(a)-(e), show the profile of mean values of story drifts for 4-, 6-, 8-, 10- and 12- story frames for suite of DBE ground motions. As shown in Figs. 9(a)-(e), rocking fames and fixed base frames have similar deformation elevation as the number of stories increase, and rocking frames experienced less remarkable changes along the frames height. In other words, in rocking frames, the distribution of inter story drifts is uniform over the frames height. This result is in line with Rahgozar *et al*. (2016). According to Fig. 9, RZBFs have 20% less inter story drifts compared with RCBFs as a result of the added zipper columns. Results of 12-story frames show that the mean values of inter story drifts is almost similar (about 1.5%) for RCBF and RZBF. This would be as a result of higher modes effects. Rocking behavior of RZBF and RCBF systems caused about 50% larger inter story drifts in rocking frames in comparison with the fixed base frames. As illustrated in Fig. 9, with increasing the number of the stories in the fixed base frames, larger inter story drift occur in a single story which led to concentration of damage in a single story. The mentioned deficiency can be overcome by using rocking behavior which result in uniform distribution of inter story drifts. For all rocking frames, maximum inter story drifts are almost uniform, which confirm that the rocking behavior dominated the peak response.

Figs. 10 and 11(a)-(e) show the elevation of residual inter story drift for rocking frame and fixed base frame, respectively. The minimum and maximum inter story residual drift mean value is 0.00053% and 0.0125% for RCBF and 0.00013% and 0.01198% for RZBF,

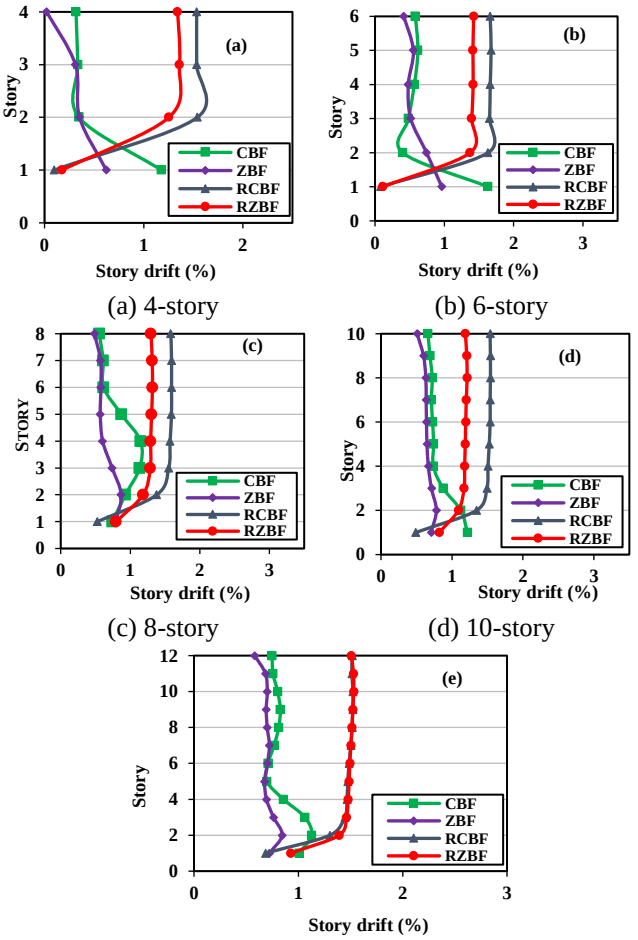

(a) 4-story (b) 6-story (c) 8-story (d) 10-story (e) 12-story

Fig. 9 Distribution of mean values of inter story drifts over the frames height for different archetypes

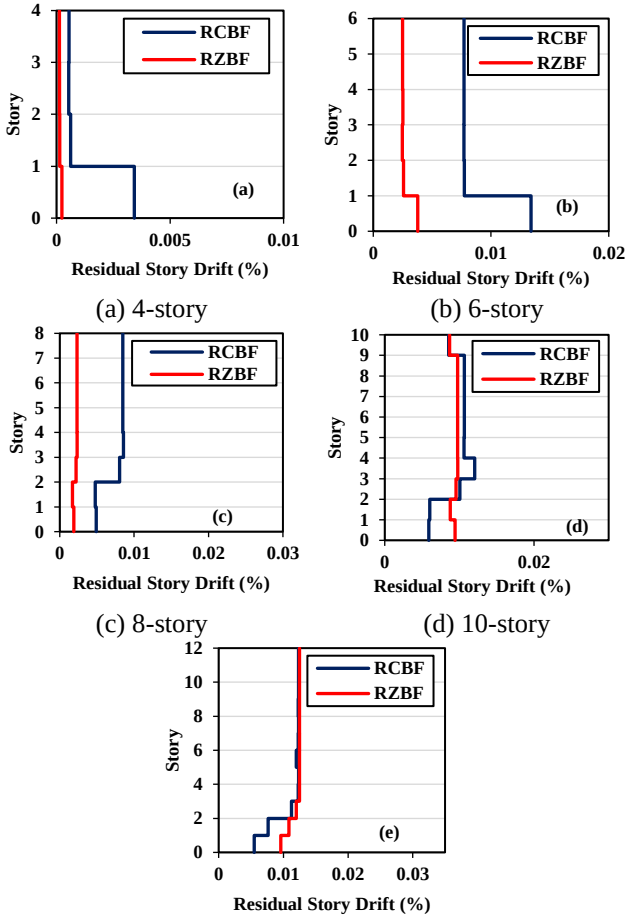

(a) 4-story (b) 6-story (c) 8-story (d) 10-story (e) 12-story

Fig. 10 Distribution of the mean values of inter story residual drifts over the frames height for rocking frames

respectively. The minimum and maximum mean values for CBF is 0.0039% and 0.207% and for ZBF is 0.0036% and 0.09%, respectively. By comparing Figs. 10 and 11 rocking frames have less residual story drifts comparing with fixed base frames.

The results of residual inter story drift show that utilizing zipper columns and rocking behavior together results in reduction of residual inter story drifts. In other words, RZBFs have better seismic performance in terms of residual story drifts. As the number of stories increase, the values of residual inter story drifts increase.

However, in all frame height fixed base frames experience larger residual inter story drifts comparing with rocking frames, for example, the mean values of residual inter story drifts of 6-story CBF is about 5 times larger than the mean values of residual inter story drifts of RCBF.

3.3 Roof drift ratio

The summary of maximum roof drift ratios for 4-, 6-, 8-, 10- and 12- story frames with different archetypes under suite of 22 far field earthquake ground motions are given in Figs. 12(a)-(e). As shown in the figures, reduced stiffness after decompression of column causes larger roof drift ratio in rocking frames compared with the fixed base frames. For example, the mean values of roof drift ratio for rocking frames are about 2-3 times larger than mean values of roof drift ratio for fixed base frames. Unlike the fixed base frames, in rocking frames, with increasing of the number of the stories, the roof drift ratio decreased.

The mean values of roof drift ratio for CBF, ZBF, RCBF and RZBF are ranged from 0.425 to 0.668%, 0.328 to 0.587%, 1.18 to 1.465% and 1.118 to 1.655%, respectively.

Residual roof drifts were computed by dividing thedifference between residual displacement of roof floor and adjacent floor by the story height. Residual roof drifts for different archetypes under suite of ground motions are presented in Fig. 13 (a) to (e). As shown in the figures rocking frames have near zero residual roof drifts in low- and mid-rise frames. This result is in consistent with previous researches (Sause *et al* 2009 and Rahgozar *et al* 2016 and 2017), validating performance of self-centering steel frame systems using hybrid simulation.

The results showed that by combining the zipper columns and rocking behavior, residual roof drifts were almost eliminated. The mean values of residual roof drifts for 4-, 6-, 8-, 10- and 12- story RZBFs are 0.000914, 0.00299, 0.003, 0.047 and 0.077%, respectively. As the number of the stories increases mean values of residual drifts for all systems increase. But the mean values of residual drifts of the frames are less than the limit values of

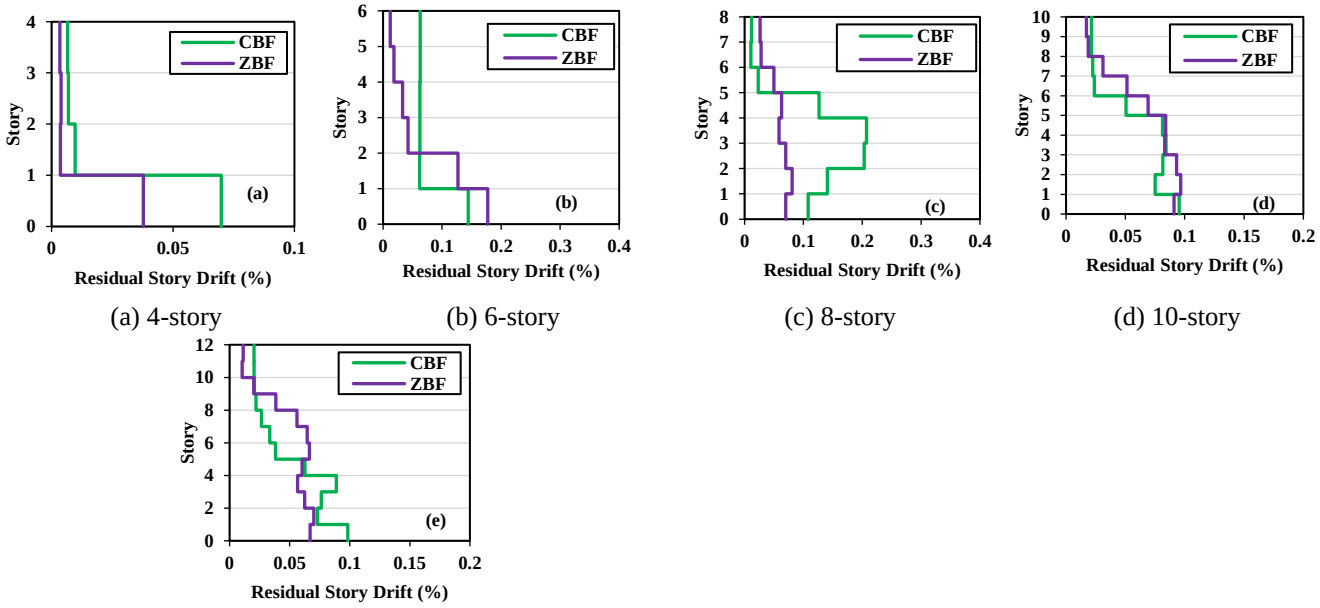

(a) 4-story (b) 6-story (c) 8-story (d) 10-story

(e) 12-story

Fig. 11 Distribution of the mean values of inter story residual drifts over the frames height for fixed base

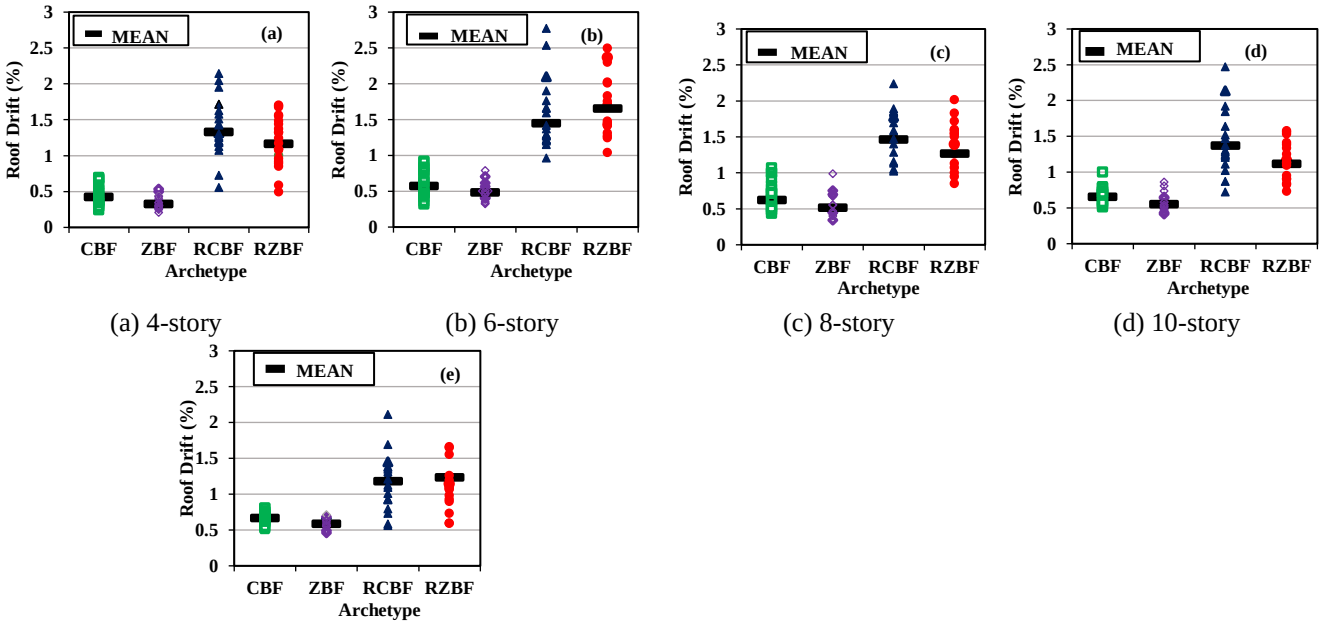

(a) 4-story (b) 6-story (c) 8-story (d) 10-story

(e) 12-story

Fig. 12 Roof drifts of different archetypes under suite of 22 earthquake records

residual drifts, 0.5 and 1% for to be repaired and rebuilt, respectively, defined by ATC-P58. Near zero residual roof drifts for rocking frames illustrated the self-centering ability of these systems which means that rocking frames experienced less damage during DBE records than fixed base systems. This result is similar to the previous studies (Dyanati *et al* 2014).

3.4 Top story braces force

Summary of peak values of top story braces force are given in Fig. 14. Top story braces forces demonstrate the responses of inertial forces of the roof, zipper columns and PT bars forces. As shown in Fig. 14, due to elastic behavior of concentrically braced frame in the rocking frame, these systems experience less unbalanced force imposing to the braces and as a result rocking frames have less brace force than fixed base frames. For example, top story brace force of CBF is 1.2-2.2 times larger than RCBF and also ZBFs have about 2.4 times larger top story brace forces compared with RZBFs. By increasing the number of stories, force of top story braces in RZBF and ZBF increase due to hat truss of these frames. With increasing the number of stories in ZBFs, need for larger top story braces increase resulting in larger force for top story braces. By using rocking behavior

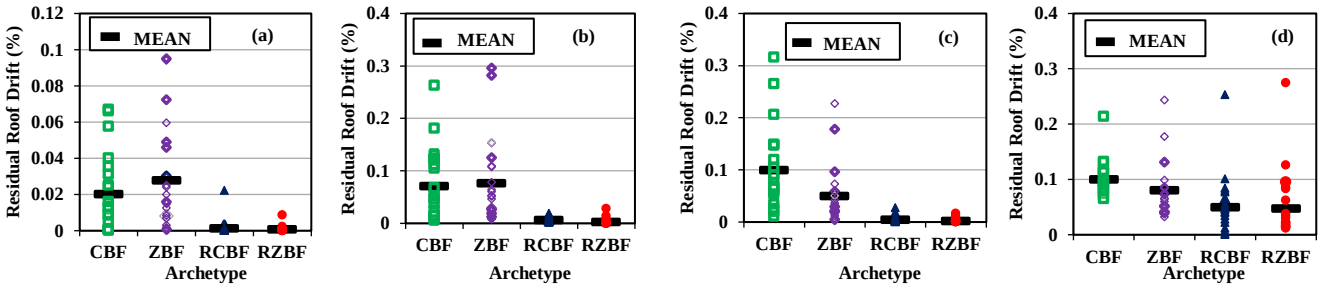

(a) 4-story (b) 6-story (c) 8-story (d) 10-story

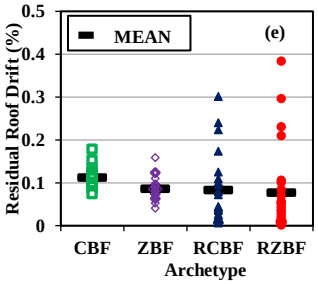

(e) 12-story

Fig. 13 Variation of residual roof drifts for different archetypes under suite of 22 earthquake records

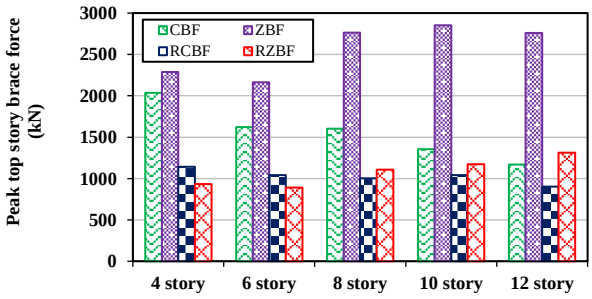

Fig. 14 Peak top story brace forces for different archetypes with various story numbers

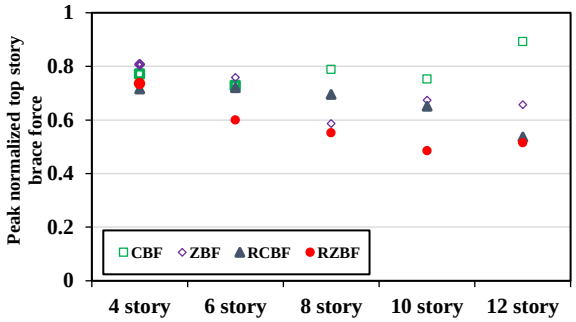

Fig. 15 Peak normalized brace force different archetypes with various story numbers

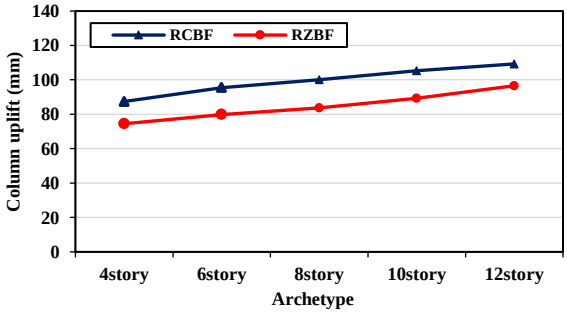

Fig. 16 Column uplift mean values for different archetypes with various story numbers

beside zipper columns, top story brace forces decreased about 60%. In other words, by using rocking concept for ZBFs in high-rise frame, the performance of ZBF in terms of top story brace forces was improved. The normalized peak top story brace forces of different archetypes are presented in Fig. 15. The values for normalized peak brace force is calculated by dividing the peak brace force to the brace force design demand. In all cases the normalized brace forces are less than 1 which indicates a conservative design demand. In the both Rocking frames (RCBF and RZBF) normalized brace forces are less than the values for the fixed base frames (CBF and ZBF), since PT bar force contribution in rocking frames dominates the brace response (Roke *et al*. 2009).Also, RZBF have the least normalized peak top story brace force than RCBF due to zipper columns contribution in distributing unbalanced force.

3.5 Column uplift

Fig. 16 presents the mean values of max column uplift of two archetypes (RCBF and RZBF) with different stories. Column uplift is determined by relative displacement between column base and column bearing. RZBFs have less column uplift than RCBFs. As shown in Fig. 16, RCBF have 20% larger column uplift in comparison with RZBF. The minimum and maximum values of column uplift for RCBF are 87.42 and 109.28 mm and for RZBF are 74.49 and 96.58 mm, respectively, which are related to 4 story and 12 story frames. Comparison between the results of column uplift and roof drift ratio show that uplift of column in rocking systems has an effect on the roof drift response.

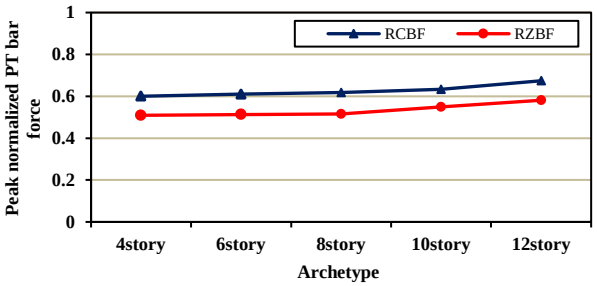

Fig. 17 Peak normalized PT bar force for rocking systems with various story numbers

With increase in the column uplift, the roof drift ratio increase in low and mid-rise frames. This result does not accommodate for high-rise frame as a result of higher mode effects.

3.6 PT bar forces

Peak normalized PT bar force (PT_{Norm}) is the ratio of maximum value of the tensile force in the PT bars to the nominal yield force of PT bars (PT_y). In fact, when PT_{Norm} is equal 1, it means that the PT force reaches the nominal yield stress. According to Fig. 17, PT bars do not yield because PT_{Norm} is less than 1 in all cases. Due to using zipper columns in RZBF, the PT bar force for RZBF is about 20% smaller than the values of PT bar force for RCBF. Zipper columns by redistributing unbalance force over the frame height reduce the PT bar forces. The maximum PT bar force for 12-story RCBF and RZBF is about 46.5% and 54% of ultimate strength of the PT bars, respectively. In this study, the ultimate Strength of the PT bars (T_u) is considered to 567 kN.

Figs. 18(a)-(b), schematically represent a combined PT bar force and column uplift response for 4-story RCBF and RZBF under r13 earthquake ground motion. The r13 record was chosen because the PT force is maximum under this record. As shown in the figures, PT bar forces are in phase with the column uplift in RCBF and RZBF. The maximum column uplift and PT bar forces under r13 record is about 59 mm and 274 kN for RCBF and 55.1 mm and 227 kN for RZBF. RZBF has smaller column uplift and PT bar force in comparison with RCBF. As previously mentioned zipper columns reduce the PT bar forces by transmitting the unbalanced force.

3.7 Base shear

The typical combined time histories of base shear and roof drift for 4 story frame under r13 record are presented in Figs. 19(a)-(b). As shown in the figures, RZBF has less roof drift ratio and base shear comparing with RCBF. Also, the time histories of base shear are consistent with time histories of roof drift ratio.

4. Conclusions

In this study, a new system comprised of zipper column and rocking concept (RZBF) was proposed in order to overcome the concentration of unbalanced force in the upper stories of the rocking systems. In the new proposed system, zipper columns by distributing the unbalance force induced by post-tensioned bars over the frame height, improve the seismic behavior. In order to evaluate seismic performance of the RZBF and its effectiveness over the height, a comparison study using four different archetypes was conducted. 4-, 6-, 8-, 10- and 12-story frames were designed. OpenSees software was used to conduct nonlinear

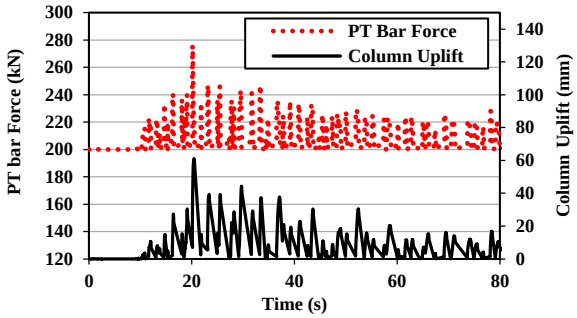

(a) RCBF

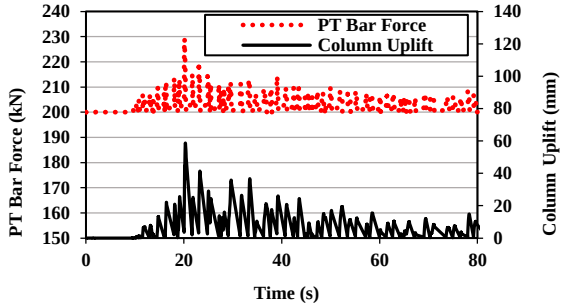

(b) RZBF

Fig. 18 Time histories of PT bar force and column uplift under r13 record

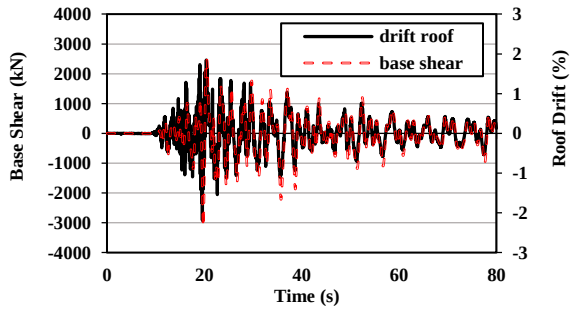

(a) RCBF

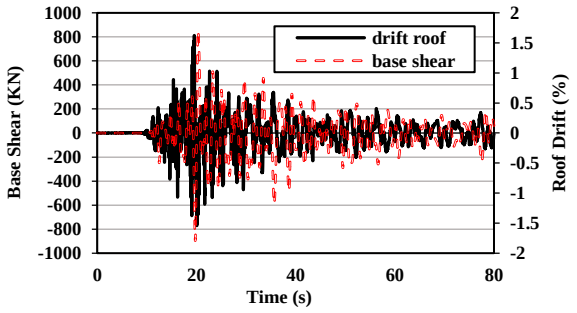

(b) RZBF

Fig. 19 Time histories of PT bar force and column uplift under r13 record

time history analysis under suite of 22 far field earthquake records to evaluate their seismic behavior. The main results are drawn as follow:

- Rocking frames experience 2-3 times larger roof drift ratio than fixed base frames. According to the residual roof drift results, rocking frames have near zero residual drifts, which indicate the self-centering behavior of these systems. As the number of story increase, the residual roof drift values increase about in all the archetypes.
- In the RZBF system, the distribution of inter story drifts is more uniform than other systems as a result of combined behavior of zipper columns and post-tensioned bars. Also, using zipper columns along with post-tensioned bars in rocking frames, improve the seismic performance of the rocking frames in terms of residual inter story drifts.
- The maximum mean values of column uplift and post-tensioed bar forces related to 12-story RZBF are about 20% less than the values for ordinary rocking system due to using zipper columns in RZBFs.
- Zipper columns in the RZBF system contribute in redistributing the unbalanced force which results in the least normalized top story brace forces in comparison with the other systems.

References

AISC Committee (2010), Specification for Structural Steel Buildings (ANSI/AISC 360-10), American Institute of Steel Construction, Chicago-Illinois.

AISC 341-10 (2010), Seismic Provisions for Structural Steel Buildings, American Institute of Steel Construction, Chicago.

Ariyaratana, C. and Fahnestock, L.A. (2011), "Evaluation of buckling-restrained braced frame seismic performance considering reserve strength", *Eng. Struct.*, **33**(1), 77-89. https://doi.org/10.1016/j.engstruct.2010.09.020.

ATC (2004), Engineering Demand Parameters for Non-Structural Components, *Report No. ATC-P58,* Applied Technology Council, Redwood City, CA.

Beck, J.L. and Skinner, R.I. (1973), "The seismic response of a reinforced concrete bridge pier designed to step", *Earth. Eng. Struct. Dyn.*, **2**(4), 343-358. https://doi.org/10.1002/eqe.4290020405.

Blebo, F.C. and Roke, D.A. (2015), "Seismic-resistant self-centering rocking core system", *Eng. Struct.,* **101**, 193-204. https://doi.org/10.1016/j.engstruct.2015.07.016.

Blebo, F.C. and Roke, D.A. (2018), "Seismic-resistant self-centering rocking core system with buckling restrained columns", *Eng. Struct.*, **173**, 372-382. https://doi.org/10.1016/j.engstruct.2018.06.117.

Chancellor, N.B. (2014), *Seismic Design and Performance of Self-Centering Concentrically-Braced Frames*, Lehigh University, USA.

Christopoulos, C., Tremblay, R., Kim, H.J. and Lacerte, M. (2008), "Self-centering energy dissipative bracing system for the seismic resistance of structures: development and validation", *J. Struct. Eng.*, **134**(1), 96-107. https://doi.org/10.1061/(ASCE)0733-9445(2008)134:1(96).

Dyanati, M., Huang, Q. and Roke, D.A. (2014), "Structural and nonstructural performance evaluation of self-centering, concentrically braced frames under seismic loading", *Structures Congress 2014*, 2393-2404. https://doi.org/10.1061/9780784413357.210.

Dyanati, M., Huang, Q. and Roke, D. (2015), "Seismic demand models and performance evaluation of self-centering and conventional concentrically braced frames", *Eng. Struct.*, **1**(84), 368-381. https://doi.org/10.1016/j.engstruct.2014.11.036.

Dyanati, M., Huang, Q. and Roke, D. (2017), "Cost-benefit evaluation of self-centring concentrically braced frames considering uncertainties", *Struct. and Infrastruc. Eng.*, **13**(5), 537-553. https://doi.org/10.1080/15732479.2016.1173070.

Eatherton, M.R., Hajjar, J.F., Deierlein, G.G., Ma, X. and Krawinkler, H. (2010), "Hybrid simulation testing of a controlled rocking steel braced frame system", *9th US National and 10 th Canadian Conference on Earthquake Engineering,* Toronto, July.

Eatherton , M.R., Ma, X., Krawinkler , H., Deierlein, G.G. and Hajjar, J.F. (2014), "Quasi-static cyclic behavior of controlled rocking steel frames", *J. Struct. Eng.*, **140**(11), https://doi.org/10.1061/(ASCE)ST.1943-541X.0001005.

Fahnestock , L.A., Sause, R., Ricles, J.M. and Lu, L.W. (2003), "Ductility demands on buckling-restrained braced frames under earthquake loading", *Earth. Eng. Eng. Vib.*, **2**(2), 255-268. https://doi.org/10.1007/s11803-003-0009-5.

Garlock, M.M., Ricles, J.M. and Sause, R. (2005), "Experimental studies of full-scale posttensioned steel connections", *J. Struct. Eng.*, **131**(3), 438-448. https://doi.org/10.1061/(ASCE)0733-9445(2005)131:3(438).

Gunnarsson,I.R. (2004), "Numerical performance evaluation of braced frame systems", Ph.D. Dissertation, University of Washington, Washington.

Henry, R.S., Sritharan, S. and Ingham, J.M. (2016), "Residual drift analyses of realistic self-centering concrete wall systems", *Earth. Struct.*, **10**(2).

Hsiao, P.C., Lehman, D.E. and Roeder, C.W. (2013), "A model to simulate special concentrically braced frames beyond brace fracture", *Earth. Eng. Struct. Dyn.*, **42**(2), 183-200. https://doi.org/10.1002/eqe.2202.

Hsiao, P.C., Lehman, D.E and Roeder, C.W. (2012), "Improved analytical model for special concentrically braced frames", *J. Construct. Steel Res.*, **1**(73), 80-94. https://doi.org/10.1016/j.jcsr.2012.01.010.

Huang, Q., Dyanati, M., Roke, D.A., Chandra, A. and Sett, K. (2018), "Economic feasibility study of self-centering concentrically braced frame systems", *J. Struct. Eng.*, **144**(8), https://doi.org/10.1061/(ASCE)ST.1943-541X.0002093.

Huckelbridge, A.A. and Clough, R.W. (1977), "Earthquake simulation tests of a nine story steel frame with columns allowed to uplift", Ph.D. dissertation, University of California, Berkeley.

Khatib, I.F., Mahin, S.A. and Pister K.S. (1988), "Seismic behavior of concentrically braced steel frames", Earthquake Engineering Research Center, University of California.

Kelly, J.M., and Tsztoo, D.F. (1977), "Earthquake simulation testing of a stepping frame with energy-absorbing devices", EERC 77-17, Earthquake Engineering Research Center, University of California, U.S.A.

Kiggins, S. and Uang, C.M. (2006), "Reducing residual drift of buckling-restrained braced frames as a dual system", *Eng. Struct.*, **28**(11), 1525-1532. https://doi.org/10.1016/j.engstruct.2005.10.023.

Kurama, Y., Pessiki, S., Sause, R. and Lu, L.W. (1999a), "Seismic behavior and design of unbonded post-tensioned precast concrete walls", *PCI J.*, **44**(3), 72-89.

Kurama, Y., Sause, R., Pessiki, S and Lu, L.W. (1999b), "Lateral load behavior and seismic design of unbonded post-tensioned precast concrete walls", *Struct. J.*, **96**(4), 622-632.

Lin, Y.C., Ricles, J., Sause, R. and Seo, C.Y. (2009), "Earthquake simulations on a self-centering steel moment resisting frame with web friction devices", *Structures Congress: Don't Mess with Structural Engineers: Expanding Our Role* (1-10), Austin, Texas, April. https://doi.org/10.1061/41031(341)149.

Liu, J. and Astaneh-Asl, A. (2004), "Moment–rotation parameters for composite shear tab connections", *J. Struct. Eng.*, **130**(9), 1371-

1380.https://doi.org/10.1061/(ASCE)0733-9445(2004)130:9(1371).
McKenna, F., Fenves, G.L. and Scott, M.H. (2000), "Open system for earthquake engineering simulation", University of California Berkeley, CA.
Ozcelik, Y., Saritas, A. and Clayton, P.M. (2016), "Comparison of chevron and suspended-zipper braced steel frames", *J. Constr. Steel Res.*, **1**(119), 169-175. https://doi.org/10.1016/j.jcsr.2015.12.019.
Pollino, M. and Bruneau, M. (2007), "Seismic retrofit of bridge steel truss piers using a controlled rocking approach.", *J. Bridge Eng.*, **12**(5), 600-610. https://doi.org/10.1061/(ASCE)1084-0702(2007)12:5(600).
Pollino, M. and Bruneau, M. (2010), "Seismic testing of a bridge steel truss pier designed for controlled rocking", *J. Struct. Eng.*, **136**(12), 1523-1532. https://doi.org/10.1061/(ASCE)ST.1943-541X.0000261.
Rahgozar, N., Moghadam, A.S., Rahgozar, N. and Aziminejad, A. (2016), "Performance evaluation of self-cenetring steel-braced frame", *Proceedings of the Institution of Civil Engineers-Structures and Buildings*, **170**(1), 3-16. https://doi.org/10.1680/jstbu.15.00136.
Rahgozar, N., Moghadam, A.S. and Aziminejad, A. (2017), "Response of self-centering braced frame to near-field pulse-like ground motions", *Struct. Eng. Mech.*, **62**(4), 497-506. https://doi.org/10.12989/sem.2017.62.4.497.
Ricles, J.M., Sause, R., Garlock, M.M. and Zhao, C. (2001), "Posttensioned seismic-resistant connections for steel frames", *J. Struct. Eng.*, **127**(2), 113-121. https://doi.org/10.1061/(ASCE)0733-9445(2001)127:2(113).
Rojas, P., Ricles, J.M. and Sause, R. (2005), "Seismic performance of post-tensioned steel moment resisting frames with friction devices", *J.l Struct. Eng.*, **131**(4), 529-540. https://doi.org/10.1061/(ASCE)0733-9445(2005)131:4(529).
Roke, D., Sause, R., Ricles, J.M., Seo, C.Y. and Lee, K.S. (2006), "Self-centering seismic-resistant steel concentrically-braced frames", *Proceedings of the 8th US National Conference on Earthquake Engineering, EERI*, San Francisco, USA, April.
Roke , D., Sause, R., Ricles, J.M. and Gonner, N. (2009), "Design concepts for damage-free seismic-resistant self-centering steel concentrically braced frames", *Structures Congress: Don't Mess with Structural Engineers: Expanding Our Role,* 1-10. Austin, Texas, April. https://doi.org/10.1061/41031(341)155.
Roke, D.A. and Hasan, M.R. (2012), "The effect of frame geometry on the seismic response of self-centering concentrically-braced frames", *Int. J. Civil. Environ. Eng.*, **6**, 140-145.
Sabelli, R., Mahin, S. and Chang C. (2003), "Seismic demands on steel braced frame buildings with buckling-restrained braces", Eng. Struct., **25**(5), 655-666. https://doi.org/10.1016/S0141-0296(02)00175-X.
Sabelli, R. (2001), "Research on improving the design and analysis of earthquake-resistant steel-braced frames", PF2000-9, EERI, Oakland, U.S.A.
Sause, R., Ricles, J.M., Roke, D., Seo, C.Y. and Lee, K.S. (2006), "Design of self-centering steel concentrically-braced frames", *Proceedings from the 4th International Conference on Earthquake Engineering*, Taipei, October.
Sause, R., Ricles, J., Roke, D., Chancellor, N. and Gonner, N. (2010), "Large-scale experimental studies of damage-free self-centering concentrically-braced frame under seismic loading", *Structures Congress*, ASCE, May. https://doi.org/10.1061/41130(369)136.
Seo, C. (2005), "Influence of ground motion characteristics and structural parameters on seismic responses of SDOF systems", Ph.D. Dissertation, Lehigh University, U.S.A.
Terzic, V. (2013), "Modeling SCB frames using beam-column elements", *OpenSees*. Abril. http://opensees.berkeley.edu.
Tremblay, R., Lacerte, M. and Christopoulos, C. (2008), "Seismic response of multistory buildings with self-centering energy dissipative steel braces", *J. Struct. Eng.*, **134**(1), 108-120. https://doi.org/10.1061/(ASCE)0733-9445(2008)134:1(108).
Uriz, P. (2008), "Toward earthquake-resistant design of concentrically braced steel-frame structures", Pacific Earthquake Engineering Research Center.
Wiebe, L., Christopoulos, C., Tremblay, R. and Leclerc, M. (2013), "Mechanisms to limit higher mode effects in a controlled rocking steel frame. 1: Concept, modelling, and low-amplitude shake table testing", *Earth. Eng. Struct. Dyn.*, **42**(7), 1053-1068. https://doi.org/10.1002/eqe.2259.
Wolski, M., Ricles, J.M. and Sause, R. (2009), "Experimental study of a self-centering beam–column connection with bottom flange friction device", *J. Struct. Eng.*, **135**(5), 479-488. https://doi.org/10.1061/(ASCE)ST.1943-541X.0000006.
Wu, D. and Lu, X.L. (2015), "Structural performance evaluation of a new energy-dissipation and light-weight rocking frame by numerical analysis and experiment", *Proceedings of the 10th Pacific Conference on Earthquake Engineering Building and Earthquake-Resilient*, November.
Yang, C.S., Leon, R.T. and DesRoches, R. (2008), "Design and behavior of zipper-braced frames", *Eng. Struct.*, **30**(4), 1092-1100. https://doi.org/10.1016/j.engstruct.2007.06.010.
Yang, C.S., Leon, R.T. and DesRoches R. (2008), "Pushover response of a braced frame with suspended zipper struts", *J. Struct. Eng.*, **134**(10), 1619-1626. https://doi.org/10.1061/(ASCE)0733-9445(2008)134:10(1619).
Zhu, S. and Zhang, Y. (2008), "Seismic analysis of concentrically braced frame systems with self-centering friction damping braces", *J. Struct. Eng.*, **134**(1), 121-131. https://doi.org/10.1061/(ASCE)0733-9445(2008)134:1(121).

CC